HHS Public Access

Author manuscript

Exp Neurol. Author manuscript; available in PMC 2016 May 01.

Published in final edited form as:

Exp Neurol. 2015 May ; 267: 209–218. doi:10.1016/j.expneurol.2015.03.009.

Molecular Regulators of Nerve Conduction - Lessons from Inherited Neuropathies and Rodent Genetic Models

Jun Li

Department of Neurology, Center for Human Genetic Research, and Vanderbilt Brain Institute, Vanderbilt University School of Medicine, and Tennessee Valley Healthcare System – Nashville VA, Nashville, Tennessee

Abstract

Myelinated nerve fibers are highly compartmentalized. Helically wrapped lipoprotein membranes of myelin are integrated with subsets of proteins specifically in each compartment to shape the physiological behavior of these nerve fibers. With the advance of molecular biology and genetics, many functions of these proteins have been revealed over the past decade. In this review, we will first discuss how action potential propagation has been understood by classical electrophysiological studies. In particular, the discussion will be concentrated on how the geometric dimensions of myelinated nerve fibers (such as internodal length and myelin thickness) may affect nerve conduction velocity. This discussion will then extend into how specific myelin proteins may shape these geometric parameters, thereby regulating action potential propagation. For instance, periaxin may specifically affect the internodal length, but not other parameters. In contrast, neuregulin-1 may affect myelin thickness, but not axon diameter or internodal length. Finally, we will discuss how these basic neurobiological observations can be applied to inherited peripheral nerve diseases.

Keywords

action potential; nerve conduction study; sensory nerve action potential; compound muscle action potential; ion channel; voltage-gated sodium channel; voltage-gated potassium channel; node of Ranvier; paranode; juxtaparanode; septate-like junction; tight junction; adherens junction; myelination; demyelination; axonal degeneration; polyneuropathy; Charcot-Marie-Tooth disease; inherited neuropathy; CMT1A; CMT2; CMTX1; hereditary neuropathy with liability to pressure palsies; HNPP; PMP22; connexin-1; Caspr

Nerve conduction study (NCS) has been one of the most important tools in diagnosing peripheral nerve diseases. Compound action potentials (CAP) are evoked by electrical stimuli delivered to both distal and proximal sites of peripheral nerves. If the recording is

Corresponding author: Jun Li, MD, PhD; Department of Neurology, Vanderbilt University School of Medicine, 1161 21th Avenue South, Nashville, TN 37232. jun.li.2@vanderbilt.edu.

made on muscles, the response is called compound muscle action potential (CMAP). Several measurements can be collected from CAP, including amplitudes of the potential and speed of the CAP propagation in different nerve segments (such as distal latency in distal nerve, conduction velocity in middle nerve segment, or F-wave latency in entire loop of peripheral nerve). Alterations in these measurements have been classified into two categories: de-/dysmyelination versus axonal loss. NCS in de-/dysmyelination shows slowed conduction velocity with prolonged distal latency and F-wave latency. Demyelination denotes a rupture or removal of fully differentiated Schwann cell membrane laminae that ensheath the axons. Dysmyelination is used for neuropathies with abnormal development of myelin, which is typically seen in patients with inherited neuropathies (such as Charcot-Marie-Tooth diseases, abbreviated as CMT). In contrast, axonal neuropathies demonstrate a decrease of CAP/CMAP amplitude with normal or minimally slowed conduction speed (Kimura, 1993).

Over many decades, studies through NCS have been descriptive, notwithstanding their clinical use. However, this nature starts to change with the advance of molecular genetics. In this review, we will discuss how human genetic mutations and rodent models may deepen or even revise our interpretation of NCS. A multi-discipline approach may soon reveal the molecular basis of NCS findings. We will discuss how these important discoveries may be translated into clinical practice.

Myelinated nerve fibers are highly compartmentalized by their unique protein architecture

Axons are either circumscribed by a single-layered Schwann cell membrane to form non-myelinated nerve fibers or wrapped by many layers of Schwann cell membranes to produce myelinated nerve fibers (Figure 1A). One Schwann cell invests many nonmyelinated axons, but the relationship between a Schwann cell and a myelinated axon is always one to one. Nerve fibers are bundled by perineurium into multiple fascicles before finally being encased by epineurium to form the whole peripheral nerve. Peri-/epineurium are formed by many peri-/epineurial cells along with collagen fibers, microvasculatures, and fibroblasts. Peri-/epineurial cells are connected by tight junctions and adherens junctions to seal the space between these cells, thereby protecting nerve fibers from being accessed by external pathogens (Peltonen et al, 2013).

Unlike the uniform “cable” of non-myelinated nerve fibers, myelinated nerve fibers are highly compartmentalized. Each Schwann cell wraps around an axon to form a segment of compact myelin that defines the territory of an internode. This wrapping is interrupted by a punctate gap, called the node of Ranvier. The node is demarcated by two paranodes on each side where Schwann cell membranes attach axolemma via a protein complex, called septate-like junctions. Immediately adjacent to the axoglial, septate-like junction, the portion of the myelin plus its interacting axolemma is called the juxtaparanode. Each compartment contains a unique set of protein constituents (Figure 1B). For instance, at the node of Ranvier, voltage-gated sodium channels (Na_v) are concentrated. Na_v interacts with neurofascin-186 and gliomedin through ankryn-G and βIV-spectrin. The paranodal region contains the Schwann cell proteins myelin-associated glycoprotein (MAG), Connexin-32 (Cx32), neurofascin-155 (Nf155), the axolemmal proteins Caspr and contactin. Nf155

interacts with Caspr and contactin to form transverse bands (at septate-like junctions) that bridge the paranodal myelin loops to the axolemma. The juxtaparanode contains voltage-gated potassium channels ($K_v1.1$ and $K_v1.2$) on the axolemma. The internode possesses the myelin structural proteins, myelin protein zero (MPZ), peripheral myelin protein-22 (PMP22), and myelin basic protein (MBP), which participate in forming the tightly-compacted myelin sheath (Scherer et al, 2002). As discussed below, dimensions of these compartments crucially affect action potential propagation. Because these aforementioned proteins are intimately integrated into the myelin, they critically affect the formation and maintenance of these myelin compartments. Changes of these proteins would alter nerve conduction.

Basic principles of action potential propagation in individual nerve fibers are shared between non-myelinated and myelinated nerve fibers

The discovery of the ionic basis of action potentials landed a Nobel Prize to Alan Hodgkin, Andrew Huxley, and John Eccles in 1963. Taking advantage of the giant axon from squid (non-myelinated), Hodgkin and Huxley observed axolemmal permeability (conductance) to K^+ ions at rest, but not to Na^+ ions. Due to intra-axonal K^+ concentration being 20 times higher than that in extracellular space, this ionic gradient establishes a resting membrane potential (around -60 to -100mV).

During action potentials, Na^+ conductance across axolemma abruptly increases about 500 times (Patton TC et al, 1965). Along with a gradient of [Na^+] from a high extracellular concentration to a low intra-axonal concentration, Na^+ influx forms the main force that drives the rising phase of action potential (depolarization). The transiently risen potential is brought back (repolarization) by inactivation of Na^+ conductance and a delayed increase of K^+ conductance (Hodgkin et al, 1990). Subsequent studies identified Na^+ and K^+ ion channels (Na_v and K_v) that are formed by transmembrane proteins and gated by membrane potentials to alter their conductance to specific ions (Catterall, 1984). The de-/repolarization will then be repeated on the axolemma adjacent to the area that was just excited, which allows the action potential to continuously propagate down the non-myelinated axon.

Despite conspicuous differences in anatomy between non-myelinated and myelinated nerve fibers, mechanism of action potentials in non-myelinated nerve fibers is largely applicable to the nodal membrane in myelinated nerve fibers. However, the outward K^+- current during repolarization (delayed rectifier) is negligible at the node of mammalian myelinated nerve fibers (Figure 2A-D). This current becomes fully recordable when the seal of paranodal myelin is acutely ruptured (Figure 2E-F), suggesting that the K^+-current is hidden under the cover of juxtaparanodal myelin (Chiu et al, 1979).

This observation brings up a question: how is the depolarized nodal membrane repolarized if the K^+-current is not available at the node? In 1982, Barrett and Barrett demonstrated a pathway that connects the nodal extracellular space and internodal periaxonal space electrophysiologically (Barrett et al, 1982). The anatomical spaces underlying the pathway have been speculated to go through Schmidt-Lanterman incisures, gap junctions and/or septate-like junctions, based on experimental evidences (Barrett *et al.*, 1982;Feder,

1971;Hirano et al, 1969;Mierzwa et al, 2010a;Rosenbluth, 2009). After the node is depolarized, the pathway allows internodal axolemmal capacitance to recharge the nodal membrane using capacitative current flowing through the pathway (Figure 2G). Moreover, outward current through K_v in the juxtaparanode can speed up the repolarization through the pathway (Chiu et al, 1999). Finally, there is slow K_v on the internodal axolemma. They are activated near the resting potential to maintain the internodal membrane potential, which contributes about 20mV to the nodal membrane resting potential (Chiu et al, 1984) likely also via the pathway. None of the mechanisms would work if the periaxonal space was perfectly sealed by the myelin.

The inward current of Na_v at an excited node has to be preserved during the nerve conduction so that there will be sufficient current available to depolarize next node. How does the myelinated nerve fiber overcome the imperfect insulation by the periaxonal pathway initially proposed by Barrett and Barrett then? This is largely achieved by internodal compact myelin. The thick myelin drastically minimizes the cost of nodal depolarizing current to charge the inner surface of internodal axolemma (transverse myelin capacitance). This capacitance allows a majority of depolarizing current to be delivered to the next node even in the presence of some myelin leakage (such as through the periaxonal pathway initially proposed by Barrett and Barrett). Due to the high density of nodal Na_v and the minimized transverse capacitance, the depolarizing current is typically five times higher than the minimum current required for action potential induction at a given node. This surplus is called the “safety factor” (Hartline et al, 2007;Rosenbluth, 2009).

Factors that affect the speed of action potential propagation

Differential diagnosis of neuropathy subtypes relies on the change of conduction speed in myelinated nerve fibers, regardless if it is expressed as distal latency, conduction velocity, or long loop latency. Thus, factors governing conduction speed are crucial to both basic and clinical neuroscience. Rushton pioneered on this issue (RUSHTON, 1951). He observed that conduction velocity is linearly proportional to the diameter of myelinated nerve fibers, myelin thickness, and internodal length over certain ranges. Subsequently, Moore et al have detailed the relative contributions of the factors in regulating conduction velocities by simulation (Moore et al, 1978). The conduction velocity is relatively sensitive to the axoplasmic conductivity, fiber diameter, and myelin transverse capacitance (Figure 2H). In contrast, it is less sensitive to the specific nodal parameters, such as nodal area, nodal capacitance, nodal Na_v-conductance (G_{Na}) or axonal constriction at the node. Interestingly, conduction velocity depends on internodal length over a small range. After that, there is little gain of conduct velocity by the increase of internodal length. Although these quantitative simulations are very helpful, these predictions lacked confirmation of experimental evidence. This is mainly due to the change of one parameter inducing co-varying of other parameters. In addition, these early studies also gave minimal considerations on paranodal contributions, presumably due to sparse knowledge about this region at that time.

Molecular dissection of factors affecting conduction velocity

With the advance of molecular genetics, it has become possible to dissect out individual proteins that are responsible for the specific anatomical parameters described in myelinated nerve fibers. These observations have deepened our understanding on molecular basis regulating nerve conduction.

1. Neuregulin-1 (Nrg1) is a master regulator of myelin thickness

Nrg1 is primarily represented by four subtypes (I-IV) in the peripheral nervous system. All four subtypes share an extracellular epidermal growth factor-like (EGF) domain. When Nrg1 binds to its receptor, the erbB2/3 dimer, the EGF domain is sufficient to activate the receptor (Nave et al, 2006), and triggers a cascade of signaling events, including activation of Akt (Nave *et al.*, 2006;Taveggia et al, 2005). Different subtypes of Nrg1 are defined by their unique N-termini adjacent to the EGF domain. While subtypes I, II and IV carry an immunoglobin (Ig)-like domain in their N-termini, type-III Nrg1 has a cysteine-rich domain (CRD) in the N-terminus (Falls, 2003). Axon-derived type-III Nrg1 appears to be the primary molecule that determines myelin thickness during the development of PNS (Figure 3A). When the comparison was made between wild-type and *Nrg1*+/−/*ErbB2*+/− mouse nerves, there was a 23.5% reduction of conduction velocity in the mutants (Michailov et al, 2004;Taveggia *et al.*, 2005). This correlates with a 19.7% increase of g-ratio (decrease of myelin thickness), but there is no change of internodal length and axonal diameter in the mutants. Interestingly, in a separate study, the disk large homolog-1 (Dlg1) directly interacts with PTEN to form a negative feedback preventing Schwann cells from hypermyelination (Cotter et al, 2010). Taken together, genetic manipulation in these studies isolates a single factor – myelin thickness, and confirms its effect on conduction velocity.

2. Periaxin is required for internodal length

A similar success has been achieved in internodal length. Periaxin forms protein complexes with dystrophin-related protein-1 (DRP2) and dystroglycan. This protein complex regulates the formation of Cajal tunnels, which are patent micro-cytoplasmic bands on the superficial layer of myelinating Schwann cells. Recessive mutations of periaxin have been shown to cause CMT4F with severely decreased conduction velocity. After their initial discovery that periaxin may regulate internodal length in *Prx*−/− mice (Court FA et al, 2004), the same group of investigators engineered a mouse that expresses periaxin without its PDZ domain at its n-terminal (Wu et al, 2012). This mutant exhibits shortened internodal length with preserved axonal diameter and myelin thickness (Figure 3A). At 3 weeks of age, conduction velocity in mutants decreased by >50% of that in wild-type mice. The internodal length was gradually elongated along with the increase of conduction velocity. However, the elongation reached a “flat maximum”, beyond which no further gain in conduction velocity occurred.

3. Neurofilament light chain critically affects axonal diameter

In a transgenic mouse that sequestered neurofilaments in neuronal cell bodies, axonal diameter only reached about 50% of norm in the sciatic nerves (Figure 3A). This was associated with a decrease of conduction velocity by 35% of the norm at 3 months of age. In contrast, internodal length, myelin thickness, myelin periodicity, and nodal structure were all

preserved in the mutant peripheral nerves (Perrot et al, 2007). Interestingly, autosomal recessive mutations in the human neurofilament light subunit (*NEFL*) gene resulted in conduction velocities around 20 m/s in patients (10-20 years of age) with CMT (Yum et al, 2009).

4. Function of septate-like junction carries many promises but is still a matter of debate

Septate-like junctions are situated between paranodal myelin loops and axolemma. The protein constituents of the junction include Nf155 at the tips of paranodal myelin loops and Caspr and contactin on the axolemma. The extracellular domains of the three proteins form hetero-oligomers that bridge the paranodal myelin loop and axolemma. Under freeze fracture EM, septate-like junctions appear to have many ridges (also called transverse bands) spiraling along the paranodal axolemma. Between the ridges, there are tiny tunnels that are patent between periaxonal space and the node of Ranvier (Rosenbluth, 2009).

Classical experiments in Figure 2 suggest that septate-like junctions may have sealed the space between the paranodal myelin loop and axolemma. This would also restrict the nodal area and thereby the nodal capacitance. A large nodal capacitance would demand excessive charges and thereby compromise the safety factor (Ritchie, 1995). The seal by septate-like junctions would prevent the depolarizing-current from shunting through the juxtaparanodal K_V that is normally covered under the juxtaparanodal myelin. This explained why the repolarizing K_V-current was absent when the action potential was recorded from the mammalian node of Ranvier (Chiu et al, 1980). Indeed, the removal of any of 3 septate-like junction proteins (Caspr, contactin or Nf155) in knockout mice detaches paranodal myelin loops from the axolemma (Bhat et al, 2001;Boyle et al, 2001;Sherman et al, 2005). All of these mice showed a conspicuous decrease of conduction velocities in mutant peripheral nerves.

However, discovery of the periaxonal pathway initially by Barrett and others clearly indicates that paranodal myelin and septate-like junctions are not perfectly sealed (Barrett *et al.*, 1982;Rosenbluth, 2009). The functional significance of this permeability has been discussed above. This permeability is further substantiated by fluorescent dextran tracers (Mierzwa *et al.*, 2010a). Thus, one would predict that the disruption of septate-like junctions would increase permeability to these tracers. Instead, disruption of septate-like junctions in *Caspr*−/− or *Cst*−/− mice resulted in no increase of the fluorescent tracer penetration to myelin (Rosenbluth et al, 2013). In contrast, an increase of tracer penetrance was found in *shaking* mice, yet the mouse septate-like junctions were largely preserved. These observations suggest that permeability of paranodal myelin is independent of paranodal junctions *per se*. Authors argued that it is the total length of a small tunnel (pathway 3; see Figure 2G) formed between the paranodal myelin loops and axolemma that determines the tracer penetrance.

There have been several additional lines of evidence against critical role of the seal by septate-like junctions in nerve conduction. First, during the repolarization of action potential, there is a large outward K_V-current at the node of amphibian myelinated nerve fibers. This is closely recapitulated in mammalian myelinated nerve fibers when paranodal

myelin is disrupted. Yet, this large outward current does not prevent action potentials from propagation in amphibian myelinated nerve fibers (Figure 2A-F).

Second, removal of septate-like junctions may enlarge nodal area (increase of nodal capacitance). However, the nodal area, even though it is a contributing factor, does not play any major role in nerve conduction velocity (Moore *et al.*, 1978). Note that this modeling by Moore et al does not consider molecular composition of node but the nodal area only. Changes in the former, such as reduction of nodal Na_v quantity, can decrease conduction velocity (Poliak et al, 2003). However, disruption of septate-like junctions in matured nerves may not significantly affect the nodal molecular composition. This issue has been well illustrated by findings in Nf155 conditional knockout mouse. A delayed removal of Nf155 and septate-like junctions after myelin development; it only resulted in a minimal change of conduction velocity with largely preserved nodal molecular architecture (Pillai et al, 2009). In contrast, when Nf155 was specifically deleted in Schwann cells at embryonic stage to remove septate-like junctions, these mice have slowed conduction velocity, and developed severe changes in distribution of other molecules, including Na_v dispersion out of the nodal region, K_v migration to the paranodal region, and organelle accumulation in the nodal/paranodal regions (Bhat *et al.*, 2001;Boyle *et al.*, 2001;Sherman *et al.*, 2005). Other relevant parameters, such as internodal length, have not been evaluated in these mice. All these abnormalities would affect conduction velocity. Thus, these findings suggest that septate-like junction *per se* may not be crucial for maintaining conduction velocity in matured nerve fibers. Septate-like junctions may secondarily affect conduction velocity by serving as a barrier for formation and maintenance of anatomical domains in developing myelinated nerve fibers. During the adulthood, septate-like junctions have also been suggested to stabilize axonal domains over time. In mutant mice lacking transverse bands, axonal domains deteriorate gradually (Mierzwa et al, 2010b).

Third, paranodal myelin permeability is largely affected by the pathway 3, not paranodal junction *per se* (Rosenbluth *et al.*, 2013). The size of the pathway 3 is usually affected by a group of molecules, such as junction adhesion molecule-C (JAM-C) (Scheiermann et al, 2007), that do not directly relate to the septate-like junction proteins. JAM-C forms homodimers between adjacent laminae of paranodal myelin loop that would close the extracellular spaces between myelin membranes (Figure 2G).

5. Other myelin junctions that affect myelin permeability and safety factor of action potential propagation

Septate-like junctions only involve a small fraction of the internode, thus, the effect of its seal may not be crucial if everything else is intact. However, if myelin permeability is altered in the entire internode, it would increase transverse myelin capacitance profoundly and affect nerve conduction. A typical example for this situation is segmental demyelination. Axons in the demyelinated internodes are devoid of myelin or only covered by thin myelin. Therefore, conduction velocity decreases or fails to propagate due to the drastically increased capacitance with large current shunting in the demyelinated internode (Bostock et al, 1976;Kaji, 2003). Furthermore, one may wonder what will happen to nerve

conduction if the internodal seal is compromised by disruption of internodal myelin junctions but myelin still remains intact.

Pertinent answers have been obtained by investigating hereditary neuropathy with liability to pressure palsies (HNPP). As its name denotes, this autosomal dominant inherited disorder typically presents with focal sensory loss and/or muscle weakness when peripheral nerves are challenged by mechanical stress. Gene mapping has revealed that patients with HNPP are associated with a heterozygous deletion of chromosome 17p12 (c17p12) (Chance et al, 1993). The c17p12 contains 9 genes, including peripheral myelin protein-22 (*PMP22*). Humans with a heterozygous truncation mutation of *PMP22* manifest a HNPP phenotype identical to that in patients with the heterozygous deletion of c17p12, supporting a causal role of loss of PMP22 function but not other genes in c17p12 (Li J et al, 2007;Nicholson et al, 1994). Mice with heterozygous knockout of the *Pmp22* gene recapitulate the pathology of humans with HNPP (Adlkofer et al, 1995). Application of mechanical compression on *Pmp22*+/− mouse nerves induced conduction block (failure of action potential propagation) more rapidly than that in *Pmp22*+/+ mouse nerves. This finding is well in line with the focal sensory loss and muscle weakness in HNPP patients when their nerves are exposed to mild mechanical stress (Bai et al, 2010;Li et al, 2002). Therefore, these mice have become an authentic model of HNPP.

Utilizing the *Pmp22*+/− mouse model, molecular mechanisms underlying the impaired action potential propagation in HNPP have been investigated lately (Guo et al, 2014). PMP22 is a tetra-span membrane protein. It is primarily localized in adult myelinating Schwann cells, while its expression is diffused in the developing nervous system (Li et al, 2013;Parmantier et al, 1997;Parmantier et al, 1995). Interestingly, demyelination is not found until the late stage of the disease (Bai et al., 2010). We found that deficiency of PMP22 dislocates junction protein complexes (tight junction and adherens junction, but spared septate-like junctions) in internodal and paranodal myelin. This change yields excessively permeable myelin that allows an entry of dextran molecules up to a size of 70Kd (Guo et al., 2014).

The severity of abnormally increased myelin permeability was found to vary in different nerve fibers (Guo et al., 2014), and would produce two different populations of myelinated nerve fibers. Those in the first group have severely “leaky” myelin that would shunt current out of nerve fibers, leading to failure of action potential propagation in the absence of demyelination. We call this “functional demyelination” (Figure 3B). Those in the second group have a mildly increased permeability of myelin, which would allow action potentials to propagate, but would compromise the safety factor of action potential propagation. This partially compromised safety factor would put the PMP22-deficient nerve fiber at risk to conduction failure if the fiber is challenged by additional external factors, such as mechanical stress.

There are three types of junctions in myelin, including tight junctions, adherens junctions, and septate-like junctions. The first two are often autotypic junctions between myelin laminae of the same cell. The third one is detailed above. Desmosomes were initially reported in myelin, but were later proven to be adherens junctions (Fannon et al, 1995).

Under freeze-fracture electron microscopy, tight junctions appear as micro-strands extruding out of the membrane (Tetzlaff, 1978). In the peripheral nerve myelin, these junctions are localized in non-compact myelin such as paranodal loops, Schmidt-Lanterman incisures, and inner/outer mesaxons (Poliak et al, 2002). The strands are formed by polymerization of claudins, which are a family of tetraspan membrane proteins. C-terminals of claudins interact with a group of cytoplasmic proteins containing PDZ-domains such as ZO1 or ZO2 (Itoh et al, 1999). On the other hand, these PDZ-containing proteins also interact with actins and link the tight junction strands to the cytoskeleton for junction stabilization (Hartsock et al, 2008).

A similar molecular organization is employed in adherens junctions. E-cadherins have a large glycosylated extracellular domain, a single transmembrane domain, and a cytoplasmic tail at the c-terminal that interacts with catenins (α-catenin, β-catenin and p120 catenin). α-catenins interact with actin filaments (Hartsock *et al.*, 2008).

Our observation in *Pmp22*+/− mice shows that abnormal formation and maintenance of these tight/adherens junctions in internodal myelin may significantly affect safety factors and action potential propagation.

6. Myelin lipids and their effect on myelin capacitance are a largely non-explored area

Lipids account for about 70% of the dry weight of myelin membrane. During development, there is approximately a 6,500-fold increase of membrane surface from an immature to a mature myelinated oligodendrocyte. This represents an enormous metabolic demand of lipids during the development of nervous system, but also brings vulnerability to diseases. Indeed, genetic conditions affecting synthesis of lipids frequently result in severe neurological abnormalities. For instance, mutations in a gene encoding sterol delta-7-reductase (DHCR7), the enzyme catalyzing the final step of cholesterol synthesis, cause Smith-Lemli-Opitz disease (SLOS) with reduced cholesterol levels and severe dysmyelination in the brain (Witsch-Baumgartner et al, 2000). Occasionally, SLOS develops a peripheral neuropathy with demyelination (Starck et al, 1999). When cholesterol synthesis in Schwann cells was blocked by inactivation of sequalene synthase (gene symbol *fdft1*), dysmyelination was severe. Conduction velocity was expected to be slow, but was not tested (Saher et al, 2009).

Genetic inactivation of *Pex7* in mice prevents PTS2 from entering peroxisomes, leading to a reduction of plasmalogens (glycerophospholipids with a 1-O-alkenyl ether bond at the sn-1 position of the glycerol) and an accumulation of very long chain fatty acids (VLCFA). This resulted in abnormal myelination, axonal loss and slowed conduction velocity (Brites et al, 2003;da Silva et al, 2014).

However, these findings above are difficult to be interpreted in its effect on nerve conduction due to a variety of changes secondary to primary alterations of lipid metabolism. However, results from studies of galactocerebroside (GalC) and sulfatide are helpful in this regard. Both of the lipids are highly enriched in myelin. Inactivation of a gene encoding UDP-galactose:ceramide galactosyltransferase (CGT) eliminates GalC and sulfatide in mice (Coetzee et al, 1996;Dupree et al, 1998a;Dupree et al, 1998b). Knockout of a gene encoding

cerebroside sulfotransferase (CST) eliminates sulfatide, but spares GalC (Honke et al, 2002). Both *Cgt*−/− and *Cst*−/− mice developed normal peripheral myelin thickness and compaction ultrastructurally with normal expression of compact myelin proteins. Interestingly, there was about 50% reduction of compound nerve action potential amplitude and 30-40% reduction of conduction velocity in *Cgt*−/− peripheral nerves. In contrast, *Cst*−/− mice showed normal conduction velocities in peripheral nerves (Honke *et al.*, 2002). Thus, removal of both GalC and sulfatides in *Cgt*−/− nerves, but not just sulfatides in *Cst*−/− nerves, is required to affect the conduction velocity. Alterations of molecular distribution in nodes and paranodes were found to be similar between the two mutants (Honke *et al.*, 2002). The changes of these lipids could have altered the quality of myelin.

Specific considerations of CAP

In clinical practice, NCS is recorded on the whole nerve (compound action potential = CAP), while observations of basic electrophysiology were often performed on single nerve fibers. One would have to give specific considerations when interpreting data from CAP. This issue becomes increasingly important since NCS on intact sciatic nerves is routinely done in numerous genetically manipulated mouse models.

A series of pioneer work has been done by the 1944 Nobel Prize Laureates Joseph Erlanger and Herbert Gasser to identify the constituents of CAP (designated as α, β, γ and σ in Figure 4). They also found that conduction speed and amplitude of action potential was proportional to the diameters of each nerve fiber. It was possible to assign a triangle with its height representative of action potential amplitude from a group of nerve fibers that shared similar sizes. The position of each triangle was determined by the latency of the nerve fibers. The summation of these triangles reconstructed CAP that was well matched with the trace from the actual CAP recorded from the nerve (Gasser HS et al, 1939). Therefore, CAP is equivalent to the summation of action potentials contributed by all individual nerve fibers.

Erlanger and Gasser's original intention was to use this data to explain how nerve fibers with different sizes were grouped to convey physiological signals of different modalities of sensory nerve function. However, these elegant observations are remarkably helpful in understanding clinical electrophysiology, but are hardly mentioned in the current literature.

1. In clinical NCS, CAP amplitude is obtained by the height measured from baseline to the highest point of CAP (called “negative peak amplitude”) or from the highest point to the lowest point (called “peak-to-peak amplitude). As illustrated in Figure 4, this amplitude would be mainly determined by the fibers with the largest diameters. Furthermore, we measure the distal latency and conduction velocity by using the onset of CAP. Based on Figure 4, the onset latency is determined by a group of nerve fibers with the largest diameters. This explains why NCS is only sensitive to the diseases that affect the largest myelinated nerve fibers.
2. Within each class of nerve fibers (α, β, γ and σ in Figure 4), electrophysiological property and diameter are similar between fibers, which allow them to produce a relatively narrow peak with synchrony (smoothness of the CAP curve). If some nerve fibers are demyelinated, their positions on the x-axis would have to shift

toward the right side due to the slowed conduction. The synchrony is disrupted, leading to temporal dispersion.

3. In the presence of demyelinated nerve fibers, the right shift would make the action potentials of the demyelinated nerve fibers out of the phase of the intact myelinated nerve fibers. The summation of these action potentials may cancel each other to decrease amplitude of CAP, called phase cancellation. Note that the phase cancellation should be cautiously used in mice due to the short length of peripheral nerves.

Taken together, scientific concepts from solid experiments by Erlanger and Gasser have been under-appreciated in understanding clinical electrophysiology. As discussed below, these concepts are also very helpful in understanding electrophysiological abnormalities observed in rodent models, particularly when these concepts are combined with findings from molecular genetics.

NCS behavior in inherited neuropathies

NCS is routinely performed on patients with inherited neuropathies (Charcot-Marie-Tooth disease, otherwise known as CMT), and NCS guides what genetic tests should be done to achieve a definitive diagnosis. However, it has not been well appreciated that these Mendelian-inherited disorders can reveal how mutations in single gene result in characteristic changes of human nerve conduction, thereby providing valuable information about the biology of the mutated protein. In general, patients with CMT exhibit one of five different patterns in NCS. Due to the chronicity of these diseases, a vast majority of CMT patients show absence of CAP in their sensory nerves. Therefore, these patterns of NCS changes are better detected in motor nerves.

1. Uniform slowing

This pattern was initially described in a group of CMT patients with autosomal dominant inheritance, but genetic testing was not available in 1980s (Lewis et al, 1982). In retrospect, these patients most likely had CMT1A. The uniform slowing is also seen in patients with CMT1C due to missense mutations in the *SIMPLE/LITAF* gene (Street et al, 2003). The CMT1C will be omitted from the remaining discussion due to insufficient information. The uniform slowing denotes that, while conduction velocity is decreased in these patients, the values of conduction velocity are similar between different nerves of the same limb (for example, median v.s. ulnar nerves in the right arm) or between different limbs of the same nerve (right median v.s. left median nerve). The publication did not define what the maximal difference between different nerves was to be allowed to call “uniform slowing” (Lewis *et al.*, 1982). Based on our experience, the difference is typically less than 5 m/s in most CMT1A patients, but exceptions do occur.

Sural nerve biopsies from patients with CMT1A demonstrate numerous onion bulbs. They are formed by membrane processes from multiple Schwann cells that circle around an axon but fail to form compact myelin, while one of the Schwann cells does make contact with the axon and form the compact myelin (Atanasoski et al, 2002). It has been hypothesized that this pathology is caused by repetitive demyelination and remyelination. Demyelination has

thus been considered to account for the slowed conduction velocity in CMT1A (Robertson et al, 2002;Thomas et al, 1997).

However, there are multiple lines of evidence against this assumption: (a). Many publications have documented conduction velocities in patients with CMT1A. The mean of conduction velocities was always around 20 m/s ± SD. The SD is usually small (Kaku et al, 1993;Nicholson, 1991). In contrast, active demyelination would predict highly variable conduction velocities. This is also in line with the fact that typical temporal dispersion and conduction block are hardly observable in patients with CMT1A (Lewis et al, 2000). (b). Active demyelination over years would result in a steady decline of conduction velocities, but conduction velocities show minimal changes over decades in patients with CMT1A (Birouk et al, 1997;Krajewski et al, 1999;Krajewski et al, 2000). (c). Nerve pathology studies prior to the era of genetic testing are difficult to interpret. Fortunately, a series of pathological studies have been carefully done in sural biopsies from genetically confirmed CMT1A patients. Segmental demyelination was observed, but mainly took place during the first decade and subsided after this. More importantly, detailed morphometric analysis demonstrated a significant decrease of g-ratio (suggesting an increase of myelin thickness in relating to the size of axons) in CMT1A (Gabreels-Festen et al, 1999;Gabreels-Festen et al, 1995). This finding strongly argues against active demyelination being a main pathological process in CMT1A since demyelination should increase the g-ratio (thin myelin), rather than decrease the g-ratio. Instead, these studies revealed that a loss of smallest and largest myelinated nerve fibers at the early stage of life. This leaves a group of myelinated nerve fibers that are relatively “homogenous” in their sizes. Based on the observations by Erlanger and Gasser (Figure 4), the clustering of these nerve fibers with similar sizes would produce similar conduction velocities in all peripheral nerves – uniform slowing. (d). We have utilized newly established human skin biopsy techniques to examine this issue (Li et al, 2005;Saporta et al, 2009). In a group of adults with CMT1A, no segmental demyelination was found. Interestingly, the internodal length was shortened in the CMT1A patients, which would contribute to the slowing of conduction velocity (Figure 3A).

Taken together, it is reasonable to speculate that there is an impaired development of CMT1A Schwann cells, leading to failure of nerve fibers to achieve diverse sizes and adequate internodal length likely due to inadequate production of Neuregulin-I from developing Schwann cells (Fledrich et al, 2014). These abnormalities would explain the uniform slowing in CMT1A (Lewis *et al.*, 1982). Thus, CMT1A is probably better termed as a dysmyelinating disease, rather than a demyelinating disease. How abnormal development of Schwann cells takes place in CMT1A still remains to be answered.

2. Extreme slowing

A subset of CMT patients develops congenital hypomyelination. They show severely delayed developmental milestones or never achieve the expected milestones. Conduction velocities are extremely slow and often below 10m/s. This severe phenotype was called Dejerine Sottas syndrome in early literature. This group of diseases is typically caused by missense mutations in one of several myelin genes, including *PMP22*, *myelin protein zero* (*MPZ*) or *EGR2* (Li, 2012).

In the past, patients with some missense mutations in *PMP22* were also classified as CMT1A by some investigators (Patel et al, 1992). This was largely due to some observations that suggest that over-expression of wild-type PMP22 may lead to protein aggregates similar to those aggregates in Schwann cells with *PMP22* missense mutations. The aggregates are formed primarily by oligomers of PMP22 (Dickson et al, 2002;Fortun et al, 2003;Fortun et al, 2006;Fortun et al, 2007;Niemann et al, 2000). These findings are usually derived from mice with a supernumber of *Pmp22* transgenes (*7 copies*) or with missense mutations of Trembler or Trembler-J in *Pmp22* (Fortun *et al.*, 2003;Fortun *et al.*, 2006;Fortun *et al.*, 2007;Rangaraju et al, 2010), while patients with CMT1A only harbor *3 copies* of wild-type *PMP22*. Indeed, sural biopsies from many patients with CMT1A showed no aggregates while aggregates were readily detectable in patients with Trembler or Trembler-J mutations (Hanemann et al, 2000). Furthermore, experiments using microarray have shown distinct mechanisms between gain-of-function point mutation mice (*Trembler* or *Trembler-J*) and mice with PMP22 over-expression. The former shows transcriptional changes in stress response, and the latter demonstrates alterations in Schwann cell proliferation (Giambonini-Brugnoli et al, 2005;Vigo et al, 2005). Together, this data suggests that patients with missense mutations of *PMP22* should be considered a separate entity (CMT1E) from CMT1A (Li *et al.*, 2013).

This difference is relevant to the mechanisms accounting for the extreme slowing of conduction velocities. Unlike sural biopsies from patients with CMT1A, nerve biopsies from patients with some missense mutations of *PMP22* demonstrated a robust increase of g-ratio (thin myelin) with the presence of onion bulbs. This observation in humans is well in line with studies in TrJ mice. It showed active segmental demyelination and extremely shortened internodes (as little as 20μM) (Devaux et al, 2005). Similar findings were also observed in the sural biopsies from patients with missense mutations in *MPZ* (Bai YH et al, 2006). These findings are also consistent with the extreme slowing of conduction velocities in humans with the missense mutation. This also does not exclude a contribution of failed elongation of Schwann cells during internodal development.

3. Intermediate slowing

This group of diseases is typified by CMT1X with mutations (missense mutations in a vast majority of cases) in *connexin-32* (*Cx32*). CMT1X will be the primary subject to be discussed here. Other diseases in this group are omitted due to insufficient information.

The *Cx32* gene on chromosome Xq13.1 is also called “gap junction protein beta-1 (*GJB1*)” which encodes a 32Kd protein with 283 amino acids. Six connexins form a hemichannel. Two apposed hemichannels form a functional channel that transfers molecules smaller than 1Kd. Cx32 is localized to non-compact myelin where its functional channel provides a short radial route connecting the periaxonal space to the extracellular space outside of myelin (Scherer et al, 2012).

Patients with CMT1X usually have conduction velocities ranging between 30-40 m/s, which is called “intermediate slowing”. The speed is faster than the conduction velocities in most patients with CMT1A, but slower than those in patients with an axonal type of CMT. The slowing is non-uniform and varies between different nerves. In some cases, the slowing is

associated with temporal dispersion and conduction block. These features are almost indistinguishable from those in acquired demyelinating neuropathies, such as chronic inflammatory demyelinating polyneuropathy (CIDP) (Gutierrez et al, 2000;Lewis *et al.*, 2000).

Sural nerve biopsies from patients with CMT1X demonstrated highly prevalent nodal widening (or paranodal demyelination), ranging from 10% to 40% of teased nerve fibers. In contrast, segmental demyelination was usually less than 10% of the teased nerve fibers. Onion bulbs were less prevalent, comparing with that in CMT1A nerves. G-ratio was significantly decreased, suggesting a decreased myelin thickness (Hahn et al, 2001;Hahn et al, 1999). Mice with *Cx32* knocked out also developed segmental demyelination (Scherer et al, 1998). All these changes are expected to reduce conduction velocity. Internodal length was not reported in these patients and mice. The milder segmental demyelination might account for the intermediate slowing, rather than the extreme slowing.

4. Multifocal slowing

This pattern is typically observed in patients with HNPP. Conduction velocities in patients with HNPP are usually normal or mildly slowed. However, there are focally decreased conduction velocities at the sites susceptible to mechanical stress, such as the ulnar nerve across the elbow, the peroneal nerve across the fibular head or the median nerve across the wrist (Li *et al.*, 2002). This pattern of nerve conduction changes is unique. Based on our experience, it predicts a positive HNPP mutation in about 70-80% of cases.

5. Axonal loss

Patients with a primary pathology of axonal loss can be either an autosomal dominant or a recessive CMT. Conduction velocities in these patients are normal or minimally reduced. In contrast, amplitudes of CAP are decreased. Clinical features and nerve conduction changes are similar among different subtypes of axonal CMT, and are not helpful in the differential diagnosis of these subtypes. Thus, this differentiation relies on the genetic testing.

There might be differences in preferentially affected nerve fiber types among subtypes of axonal CMTs, such as sensory versus motor nerves or small fibers versus large fibers. Nevertheless, the principal in Figure 4 still applies. A decrease of contributions from a group of nerve fibers would decrease the amplitude of CAP. If a disease affects the small nerve fibers first, the CAP amplitude could be normal at the initial stage until the large myelinated nerve fibers are involved. As long as a portion of large myelinated nerve fibers are functioning, the onset of CAP will not change and conduction velocity would be preserved.

In summary, change of speed of action potential propagation is a key parameter in diagnosing peripheral nerve diseases. The speed in myelinated nerve fibers is determined by a variety of factors. However, the main players involve nerve fiber diameter, axoplasmic resistance, and myelin capacitance. Within certain ranges, conduction velocity is also sensitive to internodal length. With the advance of molecular genetics, critical molecules in regulating some nerve geometric dimensions have been identified. Abnormal nerve conduction velocity is a common electrophysiological feature in inherited neuropathies.

While pathological abnormalities in these diseases have provided some explanations for the changes of conduction speed, there is still a lack of detailed molecular mechanisms accounting for these nerve conduction changes. Therefore, it would be crucial to investigate how these molecular regulators have been affected in these peripheral nerve diseases.

Acknowledgement

This research is, in part, supported by grants from NINDS (R21NS081364, R01NS066927 to J.L.) and Department of Veterans Affairs (R&D funds to J.L.).

REFERENCES

1. Adlkofer K, Martini R, Aguzzi A, Zielasek J, Toyka KV, Suter U. Hypermyelination and demyelinating peripheral neuropathy in Pmp22-deficient mice. Nat. Genet. 1995; 11:274–280. [PubMed: 7581450]
2. Atanasoski S, Scherer SS, Nave KA, Suter U. Proliferation of Schwann cells and regulation of cyclin D1 expression in an animal model of Charcot-Marie-Tooth disease type 1A. J. Neurosci. Res. 2002; 67:443–449. [PubMed: 11835311]
3. Bai YH, Ianokova E, Pu Q, Ghandour K, Levinson R, Martin JJ, Ceuterick-de Groote C, Mazanec R, Seeman P, Shy ME, Li J. R69C Mutation in P0 Gene Alters Myelination and Ion Channel Subtypes. Archives of Neurology. 2006; 63:1787–1794. [PubMed: 17172621]
4. Bai Y, Zhang X, Katona I, Saporta MA, Shy ME, O'Malley HA, Isom LL, Suter U, Li J. Conduction block in PMP22 deficiency. J Neurosci. 2010; 30:600–608. [PubMed: 20071523]
5. Barrett EF, Barrett JN. Intracellular recording from vertebrate myelinated axons: mechanism of the depolarizing afterpotential. J Physiol. 1982; 323:117–144. [PubMed: 6980272]
6. Bhat MA, Rios JC, Lu Y, Garcia-Fresco GP, Ching W, St MM, Li J, Einheber S, Chesler M, Rosenbluth J, Salzer JL, Bellen HJ. Axon-glia interactions and the domain organization of myelinated axons requires neurexin IV/Caspr/Paranodin. Neuron. 2001; 30:369–383. [PubMed: 11395000]
7. Birouk N, Gouider R, Le GE, Gugenheim M, Tardieu S, Maisonobe T, Le FN, Agid Y, Brice A, Bouche P. Charcot-Marie-Tooth disease type 1A with 17p11.2 duplication. Clinical and electrophysiological phenotype study and factors influencing disease severity in 119 cases. Brain. 1997; 120(Pt 5):813–823. [PubMed: 9183252]
8. Bostock H, Sears TA. Continuous conduction in demyelinated mammalian nerve fibers. Nature. 1976; 263:786–787. [PubMed: 995194]
9. Boyle ME, Berglund EO, Murai KK, Weber L, Peles E, Ranscht B. Contactin orchestrates assembly of the septate-like junctions at the paranode in myelinated peripheral nerve. Neuron. 2001; 30:385–397. [PubMed: 11395001]
10. Brites P, Motley AM, Gressens P, Mooyer PA, Ploegaert I, Everts V, Evrard P, Carmeliet P, Dewerchin M, Schoonjans L, Duran M, Waterham HR, Wanders RJ, Baes M. Impaired neuronal migration and endochondral ossification in Pex7 knockout mice: a model for rhizomelic chondrodysplasia punctata. Hum. Mol. Genet. 2003; 12:2255–2267. [PubMed: 12915479]
11. Catterall WA. The molecular basis of neuronal excitability. Science. 1984; 223:653–661. [PubMed: 6320365]
12. Chance PF, Alderson MK, Leppig KA, Lensch MW, Matsunami N, Smith B, Swanson PD, Odelberg SJ, Disteche CM, Bird TD. DNA deletion associated with hereditary neuropathy with liability to pressure palsies. Cell. 1993; 72:143–151. [PubMed: 8422677]
13. Chiu SY, Ritchie JM. Potassium channels in nodal and internodal axonal membane of mammalian myelinated fibres. Nature. 1980; 284:170–171. [PubMed: 6244497]
14. Chiu SY, Ritchie JM, Rogart RB, Stagg D. A quantitative description of membrane currents in rabbit myelinated nerve. J Physiol. 1979; 292:149–166. [PubMed: 314974]

15. Chiu SY, Ritson GP. On the physiological role of internodal potassium channels and the security of conduction in myelinated nerve fibers. Proceedings of Royal Society, Series B. 1984; 220:415–422.
16. Chiu SY, Zhou L, Zhang CL, Messing A. Analysis of potassium channel functions in mammalian axons by gene knockouts. J. Neurocytol. 1999; 28:349–364. [PubMed: 10739576]
17. Coetzee T, Fujita N, Dupree J, Shi R, Blight A, Suzuki K, Suzuki K, Popko B. Myelination in the absence of galactocerebroside and sulfatide: normal structure with abnormal function and regional instability. Cell. 1996; 86:209–219. [PubMed: 8706126]
18. Cotter L, Ozcelik M, Jacob C, Pereira JA, Locher V, Baumann R, Relvas JB, Suter U, Tricaud N. Dlg1-PTEN interaction regulates myelin thickness to prevent damaging peripheral nerve overmyelination. Science. 2010; 328:1415–1418. [PubMed: 20448149]
19. Court FA, Sherman DL, Pratt T, Garry EM, Ribchester RR, Cottrell DF, Fleetwood-Walker SM, Brophy PJ. Restricted growth of Schwann cells lacking Cajal bands slows conduction in myelinated nerves. Nature. 2004; 431:191–195. [PubMed: 15356632]
20. da Silva TF, Eira J, Lopes AT, Malheiro AR, Sousa V, Luoma A, Avila RL, Wanders RJ, Just WW, Kirschner DA, Sousa MM, Brites P. Peripheral nervous system plasmalogens regulate Schwann cell differentiation and myelination. J. Clin. Invest. 2014; 124:2560–2570. [PubMed: 24762439]
21. Devaux JJ, Scherer SS. Altered ion channels in an animal model of Charcot-Marie-Tooth disease type IA. J Neurosci. 2005; 25:1470–1480. [PubMed: 15703401]
22. Dickson KM, Bergeron JJ, Shames I, Colby J, Nguyen DT, Chevet E, Thomas DY, Snipes GJ. Association of calnexin with mutant peripheral myelin protein-22 ex vivo: a basis for “gain-of-function” ER diseases. Proc. Natl. Acad. Sci. U. S. A. 2002; 99:9852–9857. [PubMed: 12119418]
23. Dupree JL, Coetzee T, Blight A, Suzuki K, Popko B. Myelin galactolipids are essential for proper node of Ranvier formation in the CNS. J. Neurosci. 1998a; 18:1642–1649. [PubMed: 9464989]
24. Dupree JL, Coetzee T, Suzuki K, Popko B. Myelin abnormalities in mice deficient in galactocerebroside and sulfatide. J. Neurocytol. 1998b; 27:649–659. [PubMed: 10447239]
25. Falls DL. Neuregulins: functions, forms, and signaling strategies. Exp. Cell Res. 2003; 284:14–30. [PubMed: 12648463]
26. Fannon AM, Sherman DL, Ilyina-Gragerova G, Brophy PJ, Friedrich VL Jr. Colman DR. Novel E-cadherin-mediated adhesion in peripheral nerve: Schwann cell architecture is stabilized by autotypic adherens junctions. J. Cell Biol. 1995; 129:189–202. [PubMed: 7698985]
27. Feder N. Microperoxidase. An ultrastructural tracer of low molecular weight. J. Cell Biol. 1971; 51:339–343. [PubMed: 4106859]
28. Fledrich R, Stassart RM, Klink A, Rasch LM, Prukop T, Haag L, Czesnik D, Kungl T, Abdelaal TA, Keric N, Stadelmann C, Bruck W, Nave KA, Sereda MW. Soluble neuregulin-1 modulates disease pathogenesis in rodent models of Charcot-Marie-Tooth disease 1A. Nat. Med. 2014; 20:1055–1061. [PubMed: 25150498]
29. Fortun J, Dunn WA Jr. Joy S, Li J, Notterpek L. Emerging role for autophagy in the removal of aggresomes in Schwann cells. J Neurosci. 2003; 23:10672–10680. [PubMed: 14627652]
30. Fortun J, Go JC, Li J, Amici SA, Dunn WA Jr. Notterpek L. Alterations in degradative pathways and protein aggregation in a neuropathy model based on PMP22 overexpression. Neurobiol. Dis. 2006; 22:153–164. [PubMed: 16326107]
31. Fortun J, Verrier JD, Go JC, Madorsky I, Dunn WA, Notterpek L. The formation of peripheral myelin protein 22 aggregates is hindered by the enhancement of autophagy and expression of cytoplasmic chaperones. Neurobiol. Dis. 2007; 25:252–265. [PubMed: 17174099]
32. Gabreels-Festen A, Wetering RV. Human nerve pathology caused by different mutational mechanisms of the PMP22 gene. Ann. N. Y. Acad. Sci. 1999; 883:336–343. [PubMed: 10586258]
33. Gabreels-Festen AA, Bolhuis PA, Hoogendijk JE, Valentijn LJ, Eshuis EJ, Gabreels FJ. Charcot-Marie-Tooth disease type 1A: morphological phenotype of the 17p duplication versus PMP22 point mutations. Acta Neuropathol. 1995; 90:645–649. [PubMed: 8615087]
34. Gasser HS, Grundfest H. Axon diameter in relation to the spike dimentions and conduction velocity in Mammalian A fibers. American Journal of Physiology. 1939; 127:393–414.

35. Giambonini-Brugnoli G, Buchstaller J, Sommer L, Suter U, Mantei N. Distinct disease mechanisms in peripheral neuropathies due to altered peripheral myelin protein 22 gene dosage or a Pmp22 point mutation. Neurobiol. Dis. 2005; 18:656–668. [PubMed: 15755691]
36. Guo J, Wang L, Zhang Y, Wu J, Arpag S, Hu B, Imhof BA, Tian X, Carter BD, Suter U, Li J. Abnormal junctions and permeability of myelin in PMP22-deficient nerves. Ann. Neurol. 2014; 75:255–265. [PubMed: 24339129]
37. Gutierrez A, England JD, Sumner AJ, Ferer S, Warner LE, Lupski JR, Garcia CA. Unusual electrophysiological findings in X-linked dominant Charcot-Marie-Tooth disease. Muscle Nerve. 2000; 23:182–188. [PubMed: 10639608]
38. Hahn AF, Ainsworth PJ, Bolton CF, Bilbao JM, Vallat JM. Pathological findings in the x-linked form of Charcot-Marie-Tooth disease: a morphometric and ultrastructural analysis. Acta Neuropathol. 2001; 101:129–139. [PubMed: 11271367]
39. Hahn AF, Bolton CF, White CM, Brown WF, Tuuha SE, Tan CC, Ainsworth PJ. Genotype/phenotype correlations in X-linked dominant Charcot-Marie-Tooth disease. Ann. N. Y. Acad. Sci. 1999; 883:366–382. [PubMed: 10586261]
40. Hanemann CO, D'Urso D, Gabreels-Festen AA, Muller HW. Mutation-dependent alteration in cellular distribution of peripheral myelin protein 22 in nerve biopsies from Charcot-Marie-Tooth type 1A. Brain. 2000; 123(Pt 5):1001–1006. [PubMed: 10775544]
41. Hartline DK, Colman DR. Rapid conduction and the evolution of giant axons and myelinated fibers. Curr. Biol. 2007; 17:R29–R35. [PubMed: 17208176]
42. Hartsock A, Nelson WJ. Adherens and tight junctions: structure, function and connections to the actin cytoskeleton. Biochim. Biophys. Acta. 2008; 1778:660–669. [PubMed: 17854762]
43. Hirano A, Dembitzer HM. The transverse bands as a means of access to the periaxonal space of the central myelinated nerve fiber. J. Ultrastruct. Res. 1969; 28:141–149. [PubMed: 5791690]
44. Hodgkin AL, Huxley AF. A quantitative description of membrane current and its application to conduction and excitation in nerve. 1952 Bull. Math. Biol. 1990; 52:25–71.
45. Honke K, Hirahara Y, Dupree J, Suzuki K, Popko B, Fukushima K, Fukushima J, Nagasawa T, Yoshida N, Wada Y, Taniguchi N. Paranodal junction formation and spermatogenesis require sulfoglycolipids. Proc. Natl. Acad. Sci. U. S. A. 2002; 99:4227–4232. [PubMed: 11917099]
46. Itoh M, Furuse M, Morita K, Kubota K, Saitou M, Tsukita S. Direct binding of three tight junction-associated MAGUKs, ZO-1, ZO-2, and ZO-3, with the COOH termini of claudins. J. Cell Biol. 1999; 147:1351–1363. [PubMed: 10601346]
47. Kaji R. Physiology of conduction block in multifocal motor neuropathy and other demyelinating neuropathies. Muscle Nerve. 2003; 27:285–296. [PubMed: 12635114]
48. Kaku DA, Parry GJ, Malamut R, Lupski JR, Garcia CA. Nerve conduction studies in Charcot-Marie-Tooth polyneuropathy associated with a segmental duplication of chromosome 17. Neurology. 1993; 43:1806–1808. [PubMed: 8414036]
49. Kimura J. Consequences of peripheral nerve demyelination: basic and clinical aspects. Can. J Neurol. Sci. 1993; 20:263–270. [PubMed: 8313241]
50. Krajewski K, Turansky C, Lewis R, Garbern J, Hinderer S, Kamholz J, Shy ME. Correlation between weakness and axonal loss in patients with CMT1A. Ann. N. Y. Acad. Sci. 1999; 883:490–492. [PubMed: 10586281]
51. Krajewski KM, Lewis RA, Fuerst DR, Turansky C, Hinderer SR, Garbern J, Kamholz J, Shy ME. Neurological dysfunction and axonal degeneration in Charcot-Marie-Tooth disease type 1A. Brain. 2000; 123(Pt 7):1516–1527. [PubMed: 10869062]
52. Lewis RA, Sumner AJ. The electrodiagnostic distinctions between chronic familial and acquired demyelinative neuropathies. Neurology. 1982; 32:592–596. [PubMed: 6283420]
53. Lewis RA, Sumner AJ, Shy ME. Electrophysiological features of inherited demyelinating neuropathies: A reappraisal in the era of molecular diagnosis. Muscle Nerve. 2000; 23:1472–1487. [PubMed: 11003782]
54. Li J, Ghandour K, Radovanovic D, Shy RR, Krajewski KM, Shy ME, Nicholson GA. Stoichiometric alteration of PMP22 protein determines the phenotype of HNPP. Archives of Neurology. 2007; 64:974–978. [PubMed: 17620487]
55. Li J. Inherited neuropathies. Semin. Neurol. 2012; 32:204–214. [PubMed: 23117945]

56. Li J, Bai Y, Ghandour K, Qin P, Grandis M, Trostinskaia A, Ianakova E, Wu X, Schenone A, Vallat JM, Kupsky WJ, Hatfield J, Shy ME. Skin biopsies in myelin-related neuropathies: bringing molecular pathology to the bedside. Brain. 2005; 128:1168–1177. [PubMed: 15774502]
57. Li J, Krajewski K, Shy ME, Lewis RA. Hereditary neuropathy with liability to pressure palsy: the electrophysiology fits the name. Neurology. 2002; 58:1769–1773. [PubMed: 12084875]
58. Li J, Parker B, Martyn C, Natarajan C, Guo J. The PMP22 Gene and Its Related Diseases. Mol. Neurobiol. 2013; 47:673–698. [PubMed: 23224996]
59. Michailov GV, Sereda MW, Brinkmann BG, Fischer TM, Haug B, Birchmeier C, Role L, Lai C, Schwab MH, Nave KA. Axonal neuregulin-1 regulates myelin sheath thickness. Science. 2004; 304:700–703. [PubMed: 15044753]
60. Mierzwa A, Shroff S, Rosenbluth J. Permeability of the paranodal junction of myelinated nerve fibers. J. Neurosci. 2010a; 30:15962–15968. [PubMed: 21106834]
61. Mierzwa AJ, Arevalo JC, Schiff R, Chao MV, Rosenbluth J. Role of transverse bands in maintaining paranodal structure and axolemmal domain organization in myelinated nerve fibers: effect on longevity in dysmyelinated mutant mice. J. Comp Neurol. 2010b; 518:2841–2853. [PubMed: 20506478]
62. Moore JW, Joyner RW, Brill MH, Waxman SD, Najar-Joa M. Simulations of conduction in uniform myelinated fibers. Relative sensitivity to changes in nodal and internodal parameters. Biophys. J. 1978; 21:147–160. [PubMed: 623863]
63. Nave KA, Salzer JL. Axonal regulation of myelination by neuregulin 1. Curr. Opin. Neurobiol. 2006; 16:492–500. [PubMed: 16962312]
64. Nicholson GA. Penetrance of the hereditary motor and sensory neuropathy Ia mutation: assessment by nerve conduction studies. Neurology. 1991; 41:547–552. [PubMed: 2011255]
65. Nicholson GA, Valentijn LJ, Cherryson AK, Kennerson ML, Bragg TL, DeKroon RM, Ross DA, Pollard JD, McLeod JG, Bolhuis PA. A frame shift mutation in the PMP22 gene in hereditary neuropathy with liability to pressure palsies. Nat. Genet. 1994; 6:263–266. [PubMed: 8012388]
66. Niemann S, Sereda MW, Suter U, Griffiths IR, Nave KA. Uncoupling of myelin assembly and schwann cell differentiation by transgenic overexpression of peripheral myelin protein 22. J Neurosci. 2000; 20:4120–4128. [PubMed: 10818147]
67. Parmantier E, Braun C, Thomas JL, Peyron F, Martinez S, Zalc B. PMP-22 expression in the central nervous system of the embryonic mouse defines potential transverse segments and longitudinal columns. J Comp Neurol. 1997; 378:159–172. [PubMed: 9120057]
68. Parmantier E, Cabon F, Braun C, D'Urso D, Muller HW, Zalc B. Peripheral myelin protein-22 is expressed in rat and mouse brain and spinal cord motoneurons. Eur. J Neurosci. 1995; 7:1080–1088. [PubMed: 7613613]
69. Patel PI, Roa BB, Welcher AA, Schoener-Scott R, Trask BJ, Pentao L, Snipes GJ, Garcia CA, Francke U, Shooter EM, Lupski JR, Suter U. The gene for the peripheral myelin protein PMP-22 is a candidate for Charcot-Marie-Tooth disease type 1A. Nat. Genet. 1992; 1:159–165. [PubMed: 1303228]
70. Patton, TC., et al. Physiology and Biophysics. W.B. Saunders; Philadelphia: 1965.
71. Peltonen S, Alanne M, Peltonen J. Barriers of the peripheral nerve. Tissue Barriers. 2013; 1:e24956. [PubMed: 24665400]
72. Perrot R, Lonchampt P, Peterson AC, Eyer J. Axonal neurofilaments control multiple fiber properties but do not influence structure or spacing of nodes of Ranvier. J. Neurosci. 2007; 27:9573–9584. [PubMed: 17804618]
73. Pillai AM, Thaxton C, Pribisko AL, Cheng JG, Dupree JL, Bhat MA. Spatiotemporal ablation of myelinating glia-specific neurofascin (Nfasc NF155) in mice reveals gradual loss of paranodal axoglial junctions and concomitant disorganization of axonal domains. J. Neurosci. Res. 2009; 87:1773–1793. [PubMed: 19185024]
74. Poliak S, Matlis S, Ullmer C, Scherer SS, Peles E. Distinct claudins and associated PDZ proteins form different autotypic tight junctions in myelinating Schwann cells. J. Cell Biol. 2002; 159:361–372. [PubMed: 12403818]
75. Poliak S, Peles E. The local differentiation of myelinated axons at nodes of Ranvier. Nat. Rev. Neurosci. 2003; 4:968–980. [PubMed: 14682359]

76. Rangaraju S, Verrier JD, Madorsky I, Nicks J, Dunn WA Jr. Notterpek L. Rapamycin activates autophagy and improves myelination in explant cultures from neuropathic mice. J Neurosci. 2010; 30:11388–11397. [PubMed: 20739560]
77. Ritchie, J. Physiology of axon.. In: Waxman, SG.; Kocsis, JD., editors. The Axon: Structure, Function and Pathpphysiology. Oxford University Press; London, England: 1995. p. 68-96.
78. Robertson AM, Perea J, McGuigan A, King RH, Muddle JR, Gabreels-Festen AA, Thomas PK, Huxley C. Comparison of a new pmp22 transgenic mouse line with other mouse models and human patients with CMT1A. J Anat. 2002; 200:377–390. [PubMed: 12090404]
79. Rosenbluth J. Multiple functions of the paranodal junction of myelinated nerve fibers. J. Neurosci. Res. 2009; 87:3250–3258. [PubMed: 19224642]
80. Rosenbluth J, Mierzwa A, Shroff S. Molecular architecture of myelinated nerve fibers: leaky paranodal junctions and paranodal dysmyelination. Neuroscientist. 2013; 19:629–641. [PubMed: 24122820]
81. RUSHTON WA. A theory of the effects of fibre size in medullated nerve. J. Physiol. 1951; 115:101–122. [PubMed: 14889433]
82. Saher G, Quintes S, Mobius W, Wehr MC, Kramer-Albers EM, Brugger B, Nave KA. Cholesterol regulates the endoplasmic reticulum exit of the major membrane protein P0 required for peripheral myelin compaction. J Neurosci. 2009; 29:6094–6104. [PubMed: 19439587]
83. Saporta MA, Katona I, Lewis RA, Masse S, Shy ME, Li J. Shortened internodal length of dermal myelinated nerve fibres in Charcot-Marie-Tooth disease type 1A. Brain. 2009
84. Scheiermann C, Meda P, Aurrand-Lions M, Madani R, Yiangou Y, Coffey P, Salt TE, Ducrest-Gay D, Caille D, Howell O, Reynolds R, Lobrinus A, Adams RH, Yu AS, Anand P, Imhof BA, Nourshargh S. Expression and function of junctional adhesion molecule-C in myelinated peripheral nerves. Science. 2007; 318:1472–1475. [PubMed: 18048693]
85. Scherer SS, Arroyo EJ. Recent progress on the molecular organization of myelinated axons. J Peripher. Nerv. Syst. 2002; 7:1–12. [PubMed: 11939347]
86. Scherer SS, Kleopa KA. X-linked Charcot-Marie-Tooth disease. J. Peripher. Nerv. Syst. 17 Suppl. 2012; 3:9–13.
87. Scherer SS, Xu YT, Nelles E, Fischbeck K, Willecke K, Bone LJ. Connexin32-null mice develop demyelinating peripheral neuropathy. Glia. 1998; 24:8–20. [PubMed: 9700485]
88. Sherman DL, Tait S, Melrose S, Johnson R, Zonta B, Court FA, Macklin WB, Meek S, Smith AJ, Cottrell DF, Brophy PJ. Neurofascins are required to establish axonal domains for saltatory conduction. Neuron. 2005; 48:737–742. [PubMed: 16337912]
89. Starck L, Bjorkhem I, Ritzen EM, Nilsson BY, von DU. Beneficial effects of dietary supplementation in a disorder with defective synthesis of cholesterol. A case report of a girl with Smith-Lemli-Opitz syndrome, polyneuropathy and precocious puberty. Acta Paediatr. 1999; 88:729–733. [PubMed: 10447131]
90. Street VA, Bennett CL, Goldy JD, Shirk AJ, Kleopa KA, Tempel BL, Lipe HP, Scherer SS, Bird TD, Chance PF. Mutation of a putative protein degradation gene LITAF/SIMPLE in Charcot-Marie-Tooth disease 1C. Neurology. 2003; 60:22–26. [PubMed: 12525712]
91. Taveggia C, Zanazzi G, Petrylak A, Yano H, Rosenbluth J, Einheber S, Xu X, Esper RM, Loeb JA, Shrager P, Chao MV, Falls DL, Role L, Salzer JL. Neuregulin-1 type III determines the ensheathment fate of axons. Neuron. 2005; 47:681–694. [PubMed: 16129398]
92. Tetzlaff W. The development of a zonula occludens in peripheral myelin of the chick embryo. A freeze-fracture study. Cell Tissue Res. 1978; 189:187–201. [PubMed: 657237]
93. Thomas PK, Marques W Jr. Davis MB, Sweeney MG, King RH, Bradley JL, Muddle JR, Tyson J, Malcolm S, Harding AE. The phenotypic manifestations of chromosome 17p11.2 duplication. Brain. 1997; 120(Pt 3):465–478. [PubMed: 9126058]
94. Vigo T, Nobbio L, Hummelen PV, Abbruzzese M, Mancardi G, Verpoorten N, Verhoeven K, Sereda MW, Nave KA, Timmerman V, Schenone A. Experimental Charcot-Marie-Tooth type 1A: a cDNA microarrays analysis. Mol. Cell Neurosci. 2005; 28:703–714. [PubMed: 15797717]
95. Witsch-Baumgartner M, Fitzky BU, Ogorelkova M, Kraft HG, Moebius FF, Glossmann H, Seedorf U, Gillessen-Kaesbach G, Hoffmann GF, Clayton P, Kelley RI, Utermann G. Mutational spectrum

in the Delta7-sterol reductase gene and genotype-phenotype correlation in 84 patients with Smith-Lemli-Opitz syndrome. Am. J. Hum. Genet. 2000; 66:402–412. [PubMed: 10677299]

96. Wu LM, Williams A, Delaney A, Sherman DL, Brophy PJ. Increasing internodal distance in myelinated nerves accelerates nerve conduction to a flat maximum. Curr. Biol. 2012; 22:1957–1961. [PubMed: 23022068]
97. Yum SW, Zhang J, Mo K, Li J, Scherer SS. A novel recessive Nefl mutation causes a severe, early-onset axonal neuropathy. Ann. Neurol. 2009; 66:759–770. [PubMed: 20039262]

Highlights

- Speed of action potential propagation is a key parameter in diagnosing peripheral nerve diseases.
- Geometric parameters, such as internodal length, may affect nerve conduction velocity.
- Specific myelin proteins may shape the parameters, thereby regulating nerve conduction.
- These molecular regulators provide insights to the pathogenesis in inherited neuropathies.

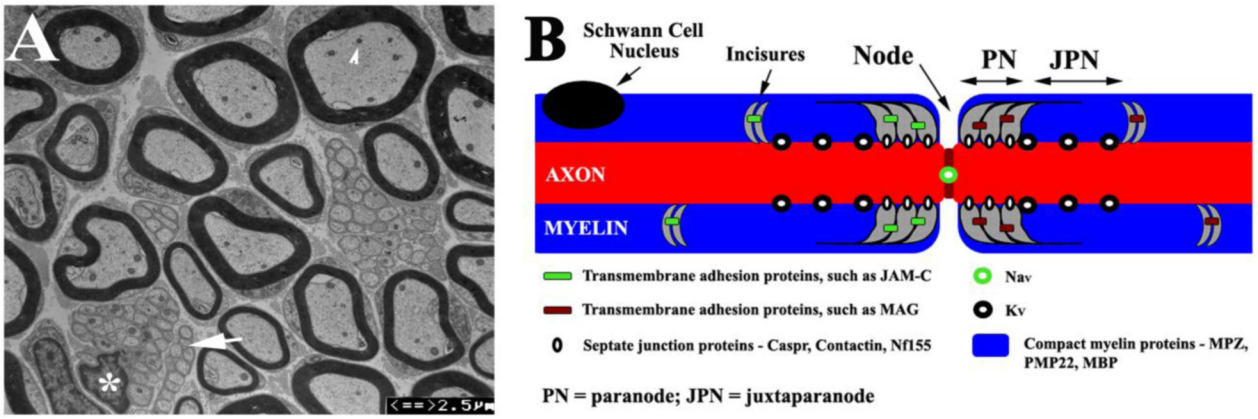

Figure 1.

(A). Transverse section of a 3-month-old mouse sciatic nerve was examined by electron microscopy. Myelinated nerve fibers showed different diameters, which varied positively with myelin thickness. Intra-axonal organelles, such as mitochondria, were visible (arrowhead). Between myelinated nerve fibers, there were Remark bundles (arrow) where a Schwann cell (its nucleus marked by an asterisk) invests a group of nonmyelinated nerve fibers. (B). A diagram illustrates the localizations of proteins on myelinated nerve fibers. Specific subsets of proteins reside in different compartments (node, paranode, juxtaparanode and compact myelin of internode) of the myelinated nerve fiber.

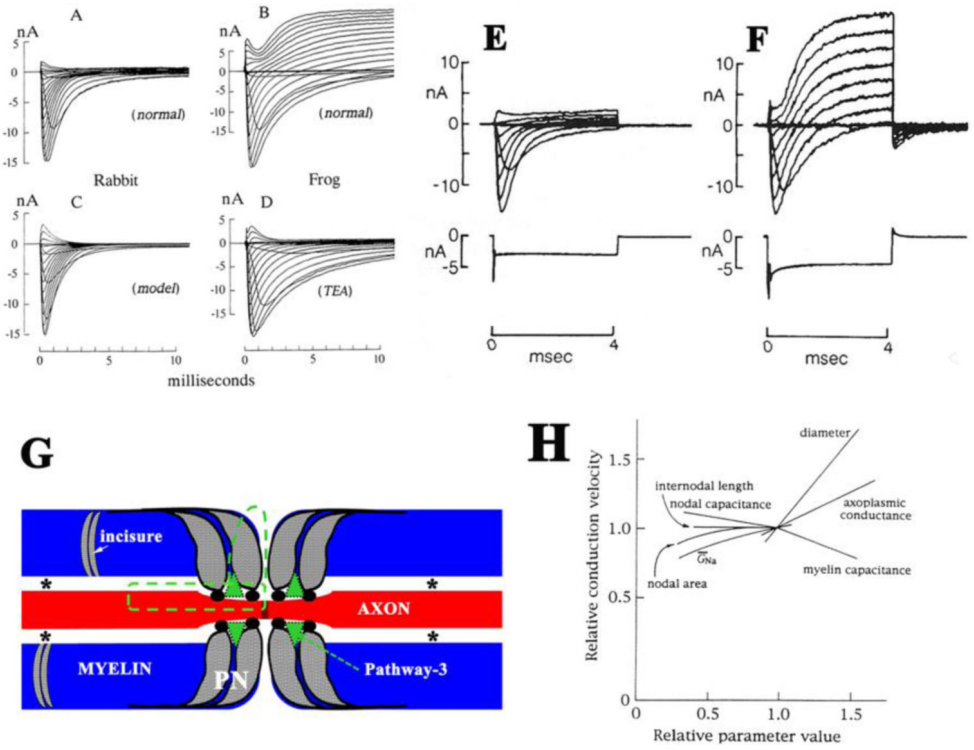

Figure 2.

A-D. Comparison of the ionic currents between rabbit and frog nodes (from Chiu et al J Physiol 1979 with permission). A. A family of ionic currents in a rabbit node generated by a series of depolarization steps starting from the holding potential, -80mV and ending at +55mV. B. The corresponding family of ionic currents in a frog node generated by a similar series of depolarization. C. A family of sodium currents calculated on the basis of the Hodgkin-Huxley parameters for sodium current in rabbit node. D. Addition of 12mM TEA-Cl to the Ringer bathing the frog node. Note that delayed rectification (potassium current) is present in the frog node but absent in the rabbit node. Ends of rabbit and frog fibers were cut in 160 and 120mM KCl respectively. B and D are from two different frog fibers. E-F. Ionic currents in a rabbit node before and after acute treatment to disrupt the myelin (from Chiu and Richie, Nature 1980 with permission). The families of currents were generated by a series of depolarization from an initial holding potential of -80mV to various test potentials in the range of -72.5mV to +62.5 in 15mV increments. E. The currents were measured in normal Locke solution after 30 minutes of myelin-loosening treatment. During this period, the outward current and the nodal capacity showed practically no change. F. The currents were measured 3 minutes after those in E (with the fiber in normal Locke solution), when the late outward current and the capacity transient current suddenly increased markedly. G. A diagram illustrates the pathway (green dot lines) that was initially proposed by Barrett and Barrett. Asterisks indicate the periaxonal spaces. Arrows point to the pathway-3 that was described (Mierzwa *et al.*, 2010a). PN = paranode. H. Relative sensitivity (defined as the ratio of percentage change of conduction velocity to percentage change in parameters above their normal values) of conduction velocity to nodal and internodal parameters in normal myelinated fibers (from Moore et al Biophysical J. 1978 with permission).

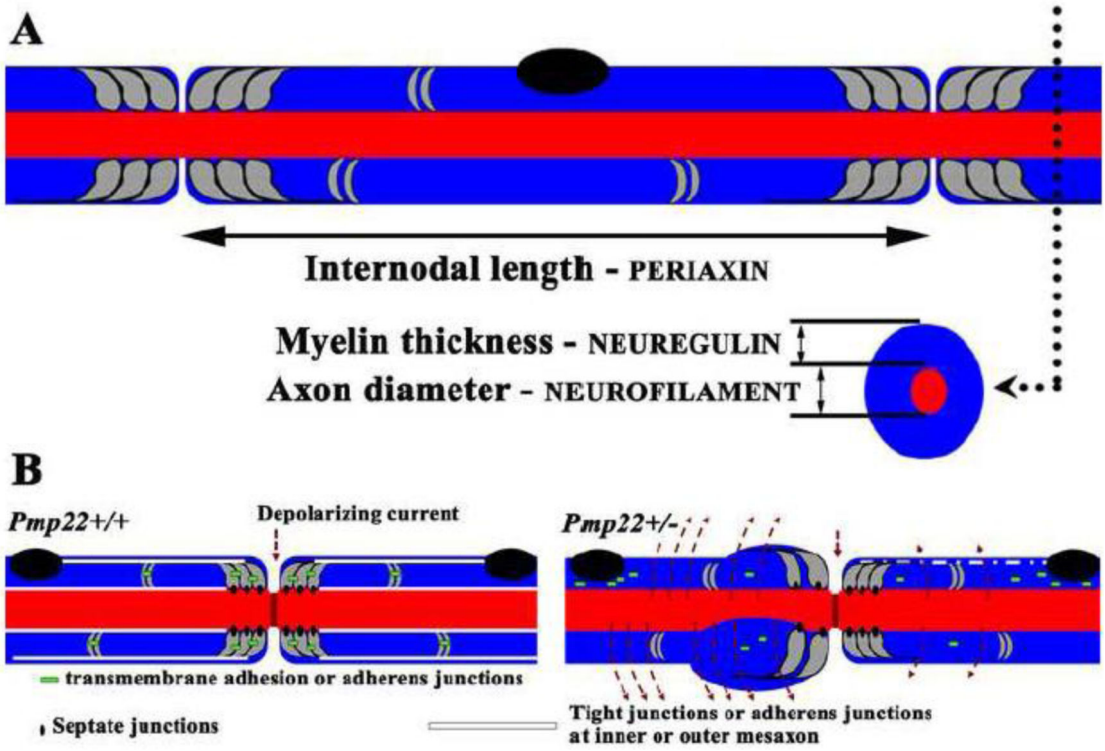

Figure 3.

A. This diagram shows the relationship between specific molecules and anatomic parameters of myelinated nerve fibers. B. This diagram is modified from the Figure 6H and I by Guo et al Ann Neurol 2014. Myelin junctions in a *Pmp22*+/+ nerve fiber are depicted in paranodes, incisures, and mesaxons. These junctions prevent axonal current from leaking out. In the figure on the right, a *Pmp22*+/− nerve fiber shows disruption or loss of junction protein complexes (tight junctions, adherens junctions or transmembrane adhesion) in paranodes, incisures, and mesaxons. These junction proteins may be found in aberrant locations, including perinuclear regions of myelinating Schwann cells. In contrast, septate-like junctions in *Pmp22*+/− nerves are still preserved. These changes increase myelin permeability that shunts current out of nerve fiber in the absence of demyelination, called “functional demyelination”.

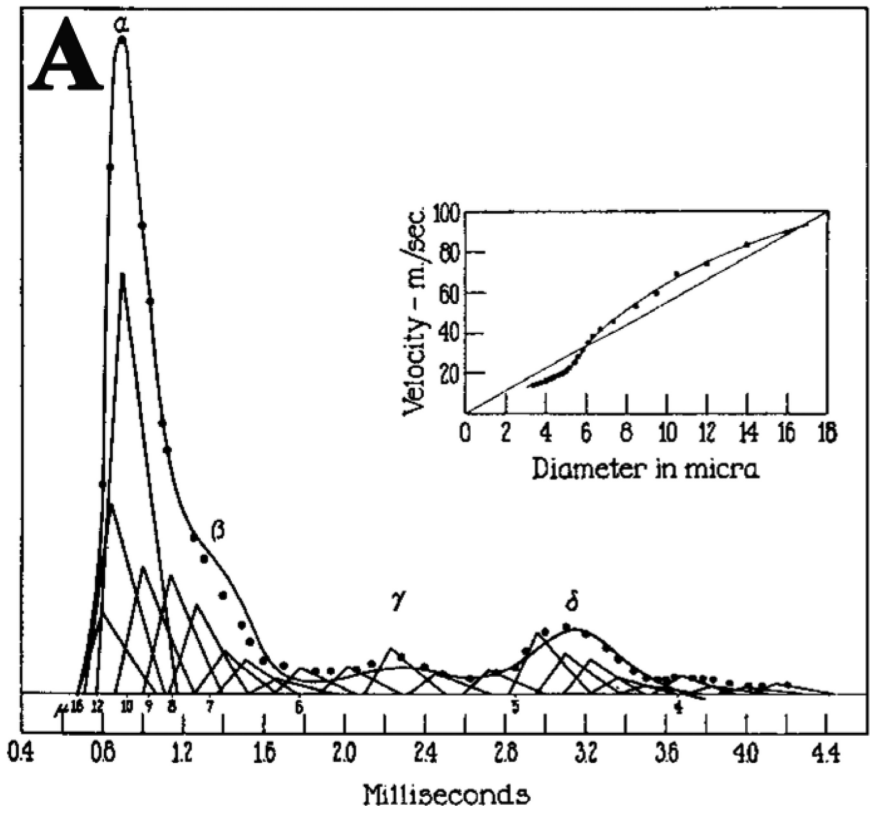

Figure 4.

Reconstruction of the action potential of the saphenous nerve of the cat (modified from Gasser et al Am J Physiol 1939 with permission). Conduction distance was 6cm. Solid-line is the recorded potential. Dotted line is the summation of triangles. The fibers larger than 16μm are grouped with the 16μm fibers.